J Mol Model (2012) 18:4427–4436
DOI 10.1007/s00894-012-1443-y

ORIGINAL PAPER

NMR and NQR study of Si-doped (6,0) *zigzag* single-walled aluminum nitride nanotube as *n* or *P* –semiconductors

Mohammad T. Baei · Ali Ahmadi Peyghan · Khadijeh Tavakoli · Ali Kazemi Babaheydari · Masoumeh Moghimi

Received: 9 March 2012 / Accepted: 18 April 2012 / Published online: 16 May 2012

Abstract Density functional theory (DFT) calculations were performed to investigate the electronic structure properties of pristine and Si-doped aluminum nitride nanotubes as *n* or *P*-semiconductors at the B3LYP/6-31G* level of theory in order to evaluate the influence of Si-doped in the (6,0) *zigzag* AlNNTs. We extended the DFT calculation to predict the electronic structure properties of Si-doped aluminum nitride nanotubes, which are very important for production of solid-state devices and other applications. To this aim, pristine and Si-doped AlNNT structures in two models (Si_N and Si_{Al}) were optimized, and then the electronic properties, the isotropic (CS^I) and anisotropic (CS^A) chemical shielding parameters for the sites of various ^{27}Al and ^{14}N atoms, NQR parameters for the sites of various of ^{27}Al and ^{14}N atoms, and quantum molecular descriptors were calculated in the optimized structures. The optimized structures, the electronic properties, NMR and NQR parameters, and quantum molecular descriptors for the Si_N and Si_{Al} models show that the Si_N model is a more reactive material than the pristine or Si_{Al} model.

Keywords Aluminum nitride nanotubes · Quantum molecular descriptors · DFT · NMR · NQR

M. T. Baei (✉)
Department of Chemistry, Azadshahr Branch,
Islamic Azad University,
Azadshahr, Golestan, Iran
e-mail: Baei52@yahoo.com

A. A. Peyghan
Young Researchers Club, Islamic Azad University,
Islamshahr Branch,
Tehran, Iran

K. Tavakoli · A. K. Babaheydari
Department of Chemistry, Sharekord Branch,
Islamic Azad University,
Sharekord, Iran

M. Moghimi
Department of Chemistry, Gonbad Kavoos Branch,
Islamic Azad University,
Gonbad Kavoos, Golestan, Iran

Introduction

Aluminum nitride (AlN) nanomaterials because of their high temperature stability, largest band gap, thermal conductivity, low thermal expansion, and resistance to chemicals and gases [1–3] are widely used in technological applications, mainly in micro and optoelectronics, such as laser diodes and solar-blind ultraviolet photodetectors and semiconductors [3]. Unlike carbon nanotubes (CNTs), aluminum nitride nanotubes (AlNNTs) exhibit electronic properties and semiconductor behavior independent of its lengths, tubular diameter and chirality. Tuning the electronic structures of the semiconducting AlNNTs for specific application is evident important in building specific electronic and mechanical devices.

Silicon is widely used in semiconductors because it remains a semiconductor at higher temperatures than the semiconductor germanium and because its native oxide is easily grown in a furnace and forms a good semiconductor/dielectric interface. Pure silicon can be doped with other elements to adjust its electrical response by controlling the number and charge (positive or negative) of current carriers. Such control is necessary for transistors, solar cells, semiconductor detectors and other semiconductor devices which are used in electronics and other high-tech applications. Silicon (Si) can replace an Al or N atom as a dopant in AlNNTs to produce p or n semiconductors. Doping of AlNNTs by Si atom may be able to yield changes in the electronic structure

properties. Therefore, investigations of the influence of Si-doping on the electronic properties of the AlNNTs are very important. Among the available techniques, Nuclear magnetic resonance (NMR) spectroscopy including isotropic and anisotropic chemical shielding (CS^I and CS^A) parameters [4] and nuclear quadrupole resonance (NQR) [5] spectroscopy are the best techniques to study the electronic structure properties of materials and can be well reproduced by density functional theory (DFT) calculations [6–9].

The electronic structure properties of AlNNTs have been theoretically studied by Mirzaei et al. [10]. They investigated just the chemical shielding (CS) parameters for the C-doped (10,0) *zigzag* AlNNT at the sites of various ^{27}Al and ^{15}N atoms, whereas the objective of the present work was to study not only the chemical shielding (CS) parameters for the Si-doped AlNNTs at the sites of various ^{27}Al and ^{15}N atoms, but also we investigated the electronic structure properties, including bond lengths, bond angles, tip diameters, dipole moments (D_M), band gaps, binding energy, and NQR parameters of ^{27}Al and ^{14}N atoms in the pristine and Si-doped AlNNT models. Moreover, we investigated the quantum molecular descriptors [11, 12] including electronic chemical potential (μ), global hardness (η), electrophilicity index (ω) [13], energy gap, global softness (S), and electronegativity (χ) of the nanotubes. Therefore, further study of the electronic properties of AlNNTs by doping process for production of solid-state devices and other applications remains interesting.

Computational methods

In this study, the electronic structure properties of the pristine and Si-doped (6,0) *zigzag* AlNNT models were studied by using density functional theory (DFT) calculations in which the ends of nanotubes were saturated by hydrogen atoms. The representative models of the (6,0) *zigzag* AlNNT has three forms, namely pristine (Fig. 1c), or with a N atom doped by a Si atom, i.e., the Si_N model (Fig. 1a) as a *p*-semiconductor, or with a Al atom doped by an Si atom, i.e., the Si_{Al} model (Fig. 1b) as a *n*-semiconductor. We investigated the influence of the Si-doping on the electronic structure properties of the (6,0) *zigzag* AlNNT, which are very important for production of solid-state devices and other applications. The hydrogenated models of the pristine (6,0) *zigzag* AlNNT and the two Si-doped AlNNT models consisted of 72 atoms with formulas $Al_{30}N_{30}H_{12}$ (pristine), $Al_{30}N_{29}H_{12}Si$ (Si_N model), and $Al_{29}N_{30}H_{16}$ Si (Si_{Al} model). In the first step, all the atomic geometrical parameters of the structures were allowed to relax in the optimization at the

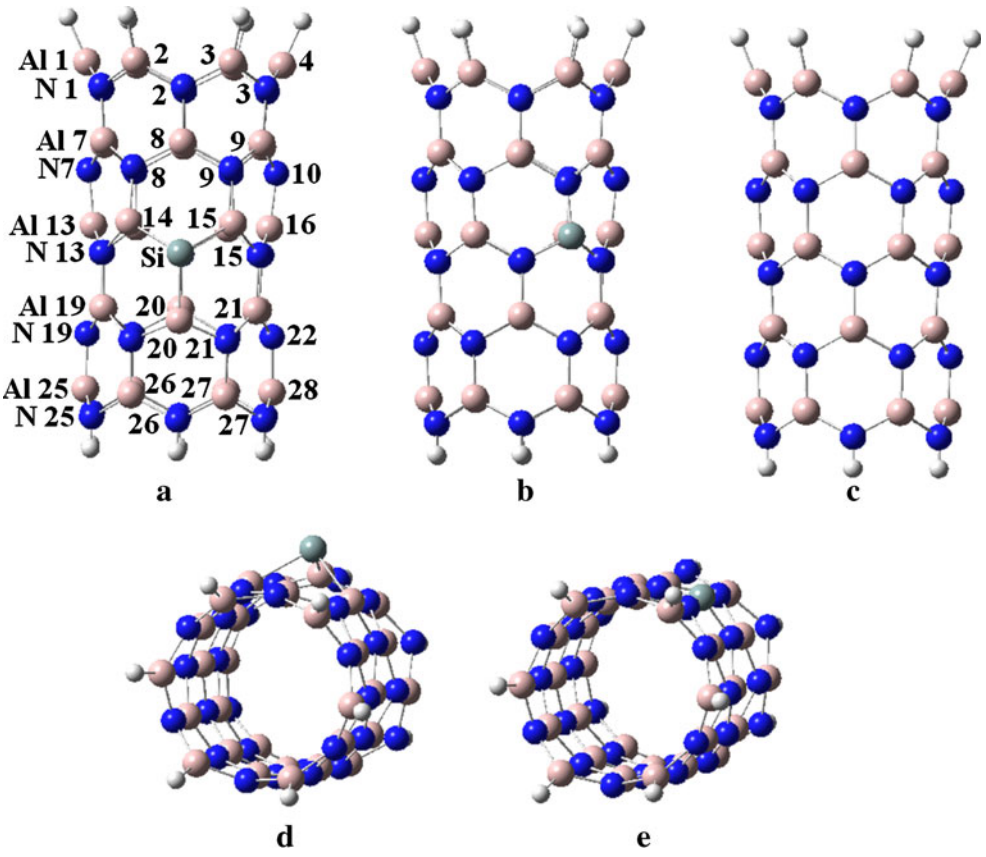

Fig. 1 (**a**) and (**b**) Two-dimensional (2D) views of the Si-doped (6,0) *zigzag* AlNNT in the Si_N and Si_{Al} models, (**c**) 2D views of pristine (6,0) *zigzag* AlNNT, and (**d**) and (**e**) Three-dimensional (3D) views of the Si-doped (6,0) *zigzag* AlNNT in the Si_N and Si_{Al} models

DFT level of B3LYP exchange functional and 6-31G* standard basis set. Then, the binding energy (*BE*) of the two Si-doped models was calculated as follows:

$$BE = [E_{\text{Si-AlNNT}} + E_{\text{N or Al}}] - [E_{\text{AlNNT}} + E_{\text{Si}}] \quad (1)$$

Where $E_{\text{Si-AlNNT}}$ was obtained from optimization of the Si-doped models, E_{AlNNT} is the energy of the optimized AlNNT structure, and E_{N}, E_{Al}, and E_{Si} are the energy of an isolated N, Al, and Si atoms. A negative *BE* denotes exothermic substitute. The structural properties of representative (6,0) *zigzag* AlNNT models are summarized in Table 1.The CS tensors of the sites of various ^{27}Al and ^{15}N atoms and NQR parameters of ^{27}Al and ^{14}N atoms were calculated for the optimized structures at the B3LYP/6-31G* level. It is noted that, when applying DFT, the B3LYP level usually gives more reliable results in comparison with experiments and is usually more convincing [14, 15]. The calculated CS tensors in the principal axis system (PAS) with order $\sigma_{33} > \sigma_{22} > \sigma_{11}$ [14, 15] were converted to measurable NMR parameters, i.e., the isotropic (CS^{I}) and anisotropic chemical shielding (CS^{A}) parameters, using Eqs. 2 and 3 [6–9]; the NMR parameters of ^{27}Al and ^{15}N

Table 1 Structural properties of representative models of the (6,0) *zigzag* AlNNT

bond	Si_N model	Si_{Al} model	Pristine	bond	Si_N model	Si_{Al} model	Pristine
Al1-N1	1.815	1.816	1.817	Al19-N20	1.817	1.817	1.816
Al2-N1	1.817	1.818	1.817	Al20-N20	1.817	1.816	1.816
Al2-N2	1.818	1.821	1.818	Al20-N21	1.817	1.810	1.816
Al3-N2	1.817	1.816	1.817	Al21-N21	1.816	1.810	1.816
Al3-N3	1.817	1.816	1.817	Al21-N22	1.824	1.816	1.816
Al4-N3	1.816	1.821	1.818	Al25-N19	1.810	1.806	1.807
Al7-N1	1.811	1.814	1.814	Al26-N20	1.807	1.810	1.807
Al8-N2	1.817	1.811	1.814	Al27-N21	1.807	1.804	1.807
Al9-N3	1.812	1.811	1.814	Al28-N22	1.809	1.810	1.807
Al7-N7	1.810	1.815	1.815	Al25-N25	1.814	1.815	1.816
Al7-N8	1.812	1.811	1.815	Al26-N25	1.809	1.816	1.816
Al8-N8	1.821	1.804	1.815	Al26-N26	1.820	1.815	1.816
Al8-N9	1.821	1.826	1.815	Al27-N26	1.820	1.815	1.815
Al9-N9	1.812	1.826	1.815	Al27-N27	1.808	1.815	1.815
Al9-N10	1.811	1.804	1.815	Al28-N27	1.814	1.816	1.816
Al13-N7	1.816	1.813	1.812	Average Al-N	1.818	1.814	1.815
Al14-N8	1.816	1.803	1.812	Al-H	1.582	1.582	1.582
Al15-N9	1.817	–	1.812	N-H	1.019	1.019	1.019
Al16-N10	1.816	1.802	1.812	Bond angles			
Al13-N13	1.834	1.816	1.818	N1-Al7-N8	119.6	118.2	119.3
Al14-N13	1.831	1.812	1.818	N2-Al8-N9	117.4	120.9	119.3
Al14-N14	–	1.821	1.818	N7-Al13-N13	121.6	118.7	119.2
Al15-N14	–	–	1.818	N8-Al14-Si	115.3	–	–
Al15-N15	1.832	–	1.818	Al14-Si-Al20	98.7	–	–
Al16-N15	1.834	1.820	1.818	N9-Si-N14	–	111.6	–
Al19-N13	1.832	1.805	1.811	Al8-N9-Si	–	123.5	–
Al20-N14	–	1.820	1.811	N20-Al20-N21	118.2	118.7	118.7
Al21-N15	1.832	1.820	1.811	N21-Al27-N27	117.6	116.5	116.8
Si-Al14	2.428	–	–	Diameter(Al-tip)/Å	6.37	6.49	6.33
Si-Al15	2.427	–	–	Diameter(N-tip)/Å	6.48	6.43	6.43
Si-Al20	2.379	–	–	D_M	12.33	11.97	12.30
Si-N9	–	1.761	–	E_T/keV	−249.272	−244.166	−242.888
Si-N14	–	1.773	–	BE/eV	6.21	−0.82	–
Si-N15	–	1.773	–	Band gap/eV	α=3.93	α=2.27	4.29
Al19-N19	1.824	1.813	1.816		β=2.45	β=4.22	

atoms for the investigated (6,0) *zigzag* AlNNT models are summarized in Table 2.

$$CS^{I}(ppm) = 1/3\ (\sigma_{11} + \sigma_{22} + \sigma_{33}), \quad (2)$$

$$CS^{A}(ppm) = \sigma_{33} - 1/2\ (\sigma_{11} + \sigma_{22}) \quad (3)$$

For NQR parameters, computational calculations do not directly return experimentally measurable NQR parameters, i.e., the nuclear quadrupole coupling constant (C_Q) and asymmetry parameter (η_Q). Therefore, Eqs. 4 and 5 were used to calculate the EFG (electric field gradient) tensors to their proportional experimental parameters; C_Q is the interaction energy of the nuclear electric quadrupole moment (eQ) with the EFG tensors at the sites of quadrupole nuclei, but the asymmetry parameter (η_Q) is a quantity of the EFG tensors that describes the deviation from tubular symmetry at the sites of quadrupole nuclei. Nuclei with I>1/2 (where I is nuclear spin angular momentum) are active in NQR spectroscopy. The calculated EFG tensor eigenvalues in the principal axis system (PAS) with order $|q_{zz}| > |q_{yy}| > |q_{xx}|$ were converted to measurable NQR parameters, i.e.; the nuclear quadrupole coupling constant (C_Q) and asymmetry parameter (η_Q), using Eqs. 4 and 5. The standard Q values [(Q (^{27}Al)=146.61 and Q (^{14}N)=20.44 mb) reported by Pyykko¨ [16] are used in Eqs. 4. The NQR parameters of ^{27}Al and ^{14}N atoms for the

Table 2 NMR parameters/ppm of the sites of various ^{27}Al and ^{15}N in representative models of the (6,0) *zigzag* AlNNTs

nucleus	Si_N model		Si_{Al} model		Pristine		nucleus	Si_N model		Si_{Al} model		Pristine	
	CS^I	CS^A	CS^I	CS^A	CS^I	CS^A		CS^I	CS^A	CS^I	CS^A	CS^I	CS^A
Al1	436.8	11.1	440.0	9.1	437.9	8.90	N1	135.7	64.5	139.5	63.0	137.5	67.3
Al2	437.7	9.5	438.5	9.7	437.9	8.90	N2	132.7	66.8	133.3	62.0	137.5	67.3
Al3	438.2	8.3	436.3	15.1	437.9	8.90	N3	136.5	65.2	132.4	62.9	137.5	67.3
Al4	437.0	10.9	438.8	9.6	437.9	8.90	N4	136.4	67.6	137.7	64.5	137.5	67.3
Al5	438.0	8.6	440.4	9.4	437.9	8.90	N5	138.5	66.5	136.5	66.0	137.5	67.3
Al6	438.5	8.5	434.4	13.9	437.9	8.90	N6	136.8	67.6	136.2	66.4	137.5	67.3
Al7	454.1	37.3	454.9	29.3	454.2	28.7	N7	147.0	55.8	173.9	26.4	173.3	26.3
Al8	458.7	33.4	455.5	45.1	454.2	28.7	N8	146.5	51.9	170.3	26.3	173.3	26.3
Al9	454.2	36.4	456.1	44.4	454.2	28.7	N9	132.7	66.8	147.6	59.0	173.3	26.3
Al10	455.2	28.2	455.8	29.7	454.2	28.7	N10	172.6	27.6	168.8	28.3	173.3	26.3
Al11	454.1	28.5	455.2	28.4	454.2	28.7	N11	172.4	24.5	174.0	28.3	173.3	26.3
Al12	455.3	27.9	454.9	28.6	454.2	28.7	N12	169.9	30.2	171.6	25.9	173.3	26.3
Al13	457.6	39.5	456.1	36.5	454.4	36.0	N13	162.8	29.2	171.6	25.2	174.5	24.0
Al14	426.4	59.1	460.3	54.2	454.4	36.0	N14	–	–	148.1	36.3	174.5	24.0
Al15	426.3	58.3	–	–	454.4	36.0	N15	162.8	29.3	147.8	33.2	174.5	24.0
Al16	457.8	38.9	462.8	52.6	454.4	36.0	N16	174.5	24.4	169.8	24.5	174.5	24.0
Al17	452.4	35.2	456.5	36.2	454.4	36.0	N17	174.4	27.9	173.6	25.8	174.5	24.0
Al18	452.9	35.2	454.6	35.9	454.4	36.0	N18	174.5	24.1	173.1	23.6	174.5	24.0
Al19	463.5	39.0	454.1	37.2	453.7	38.1	N19	185.8	25.5	184.6	30.5	183.9	28.8
Al20	435.2	43.7	455.3	29.2	453.7	38.1	N20	161.5	32.4	183.8	29.7	183.9	28.8
Al21	463.2	39.0	455.6	30.3	453.7	38.1	N21	162.2	33.8	178.7	35.0	183.9	28.8
Al22	454.3	36.1	455.0	36.2	453.7	38.1	N22	185.4	24.7	182.0	32.4	183.9	28.8
Al23	451.4	38.4	454.6	39.7	453.7	38.1	N23	183.0	31.9	184.5	32.1	183.9	28.8
Al24	453.7	36.3	454.6	39.2	453.7	38.1	N24	182.8	31.0	182.7	31.2	183.9	28.8
Al25	450.3	37.7	451.0	34.2	450.4	35.4	N25	219.8	32.2	221.3	28.8	221.4	29.6
Al26	452.3	33.1	451.4	35.6	450.4	35.4	N26	220.5	28.3	220.7	29.6	221.4	29.6
Al27	452.7	33.1	452.0	32.1	450.4	35.4	N27	220.4	32.5	220.5	30.6	221.4	29.6
Al28	450.3	37.9	451.3	34.1	450.4	35.4	N28	221.0	28.8	221.4	28.4	221.4	29.6
Al29	450.7	34.3	451.0	33.8	450.4	35.4	N29	221.3	29.5	221.1	30.6	221.4	29.6
Al30	451.4	34.5	450.4	37.1	450.4	35.4	N30	221.5	29.5	221.0	30.5	221.4	29.6

investigated models of the (6,0) *zigzag* AlNNT are summarized in Table 3.

$$C_Q\,(\mathrm{MHz}) = e^2\,Q\,q_{zz}\,h^{-1} \tag{4}$$

$$\eta_Q = |(q_{xx-}q_{yy})/q_{zz}|\;0 < \eta_Q < 1 \tag{5}$$

For the optimized AlNNT models, the quantum molecular descriptors [11, 12] including electronic chemical potential (μ), global hardness (η), electrophilicity index (ω) [13], energy gap, global softness (S), and electronegativity (χ) of the nanotubes were calculated as follows:

$$[\mu = -\chi = -(\mathrm{I}+\mathrm{A})/2], [\eta = (\mathrm{I\text{-}A})/2], \tag{6}$$

$$[\omega = \mu^2/2\eta], \text{and } [\mathrm{S} = 1/2\eta]$$

Where I ($-E_{HOMO}$) is the first vertical ionization energy and A ($-E_{LUMO}$) the electron affinity of the molecule. The electrophilicity index is a measure of electrophilic power of a molecule. When two molecules react with each other, one molecule behaves as a nucleophile while the other acts as an electrophile. Higher electrophilicity index shows higher electrophilic of a molecule. The quantum molecular descriptors were compared for the pristine and the two Si-doped models. All the calculations were carried out using a locally modified version of the GAMESS electronic structure program [17].

Results and discussion

Optimized properties of the (6,0) zigzag AlNNT models

The structural properties consisting of the Al–N bond lengths, bond angles, tip diameters, dipole moments (D_M), band gaps, energies, and binding energy for the investigated models of the (6,0) zigzag AlNNTs, are summarized in Table 1. There are two forms of the Si-doped AlNNT for the (6,0) zigzag model, namely with a N atom doped by a Si atom, i.e., the Si_N model (Fig. 1a), or with a Al atom doped by an Si atom, i.e., the Si_{Al} model (Fig. 1b). There are Al–N and Si-Al bonds in the Si_N model and Al–N and Si–N bonds in the Si_{Al} model. In Fig. 1, the atoms of the AlNNTs are numbered in order to describe the relevant structural parameters. We optimized the investigated models of the (6,0) zigzag AlNNTs at the B3LYP/6-31G* computational level. The values of the Al-N bond distances indicate that the effects of the Si dopant are important for the Al-N bond distances close to the Si-doped regions, whereas the values for other bonds do not show notable changes (see Table 1). The results presented in Table 1 indicate that the average Al–N bond lengths are almost the same in the pristine (6,0) zigzag AlNNT (Fig. 1c) and the Si_{Al} model (Fig. 1b), but different in the Si_N model (Fig. 1a) due to the influence of the Si doping on the AlNNT. In this model, the average Al–N bond length is increased from 1.815 Å in the pristine model to 1.818 Å in the Si_N model.

The bond angles shown in Table 1 indicate some difference in comparison to the pristine model, reflecting some structural deformations. Furthermore, in the pristine model, it should be noted that Al atoms relax in, while N atoms relax out, with respect to the nanotube surface, yielding different diameters of 6.33 Å for the Al mouth and 6.43 Å for the N mouth, whereas

Table 3 The ^{27}Al and ^{14}N NQR parameters in representative models of the (6,0) *zigzag* AlNNTs

nucleus	Si_N model		Si_{Al} model		Pristine		Difference betweenSi_N model and pristine		Difference betweenSi_{Al} model and pristine	
	C_Q/MHz	η_Q	C_Q/MHz	η_Q	C_Q/MHz	η_Q	ΔC_Q/MHz	$\Delta\eta_Q$	ΔC_Q/MHz	$\Delta\eta_Q$
Al1	30.52	0.16	29.97	0.13	30.42	0.15	0.10	0.01	−0.45	−0.02
Al7	25.85	0.05	25.39	0.02	25.45	0.01	0.40	0.04	−0.06	0.01
Al13	25.27	0.04	25.48	0.03	25.48	0.01	−0.21	0.03	0.00	0.02
Al19	24.78	0.10	25.62	0.04	25.56	0.04	−0.78	0.06	0.06	0.00
Al25	24.38	0.07	24.59	0.03	24.59	0.04	−0.21	0.03	0.00	−0.01
Average Al	26.16	0.08	26.21	0.05	26.30	0.05	−0.14	0.03	−0.09	0.00
N25	2.21	0.7	2.22	0.74	2.20	0.74	0.01	−0.04	0.02	0.00
N19	0.54	0.46	0.51	0.03	0.52	0.10	0.02	0.36	−0.01	−0.07
N13	0.13	0.93	0.58	0.18	0.51	0.11	−0.38	0.82	0.07	0.07
N7	0.37	0.83	0.47	0.37	0.48	0.36	−0.11	0.47	−0.01	0.01
N1	0.81	0.71	0.80	0.71	0.81	0.73	0.00	−0.02	−0.01	−0.02
Average N	0.81	0.73	0.92	0.41	0.90	0.41	−0.09	0.32	0.02	0.00

in the Si_N model (Fig. 1a), the diameters at the Al and N terminals undergo changes to 6.37 and 6.48 Å, and in the Si_{Al} model (Fig. 1b) the diameters at the Al terminal undergo changes to 6.49 Å. For the Si_N model (Fig. 1a) the diameter values are increased, whereas in the Si_{Al} model (Fig. 1b) the changes of the diameters at the N terminal remain unchanged. The results presented in Table 1 indicate that, in the two forms of the Si-doped AlNNTs, the binding energy (*BE*) for the Si_{Al} model is attractive, which is characteristic a chemisisorption process and denotes exothermic substitute, whereas for the Si_N model is not attractive and do not characterize a chemisisorption process and denotes endothermic substitute. Also, the calculated energy value for the Si_N model (Fig. 1a) is higher than that for the Si_{Al} model (Fig. 1b) and the dipole moments (D_M) of the Si-doped AlNNT structures (Fig. 1a and b) showed slight changes due to the Si-doping with respect to the pristine model.

Electronic properties of the (6,0) zigzag AlNNT models

We studied the influence of Si-doping on the electronic properties of the AlNNTs. The total densities of states (DOS) of these tubes are shown in Fig. 2. As is evident from Fig. 2, the calculated band gap of the perfect (6,0) *zigzag* AlNNT is 4.29 eV, whereas the calculated band gaps of the Si_N model (Fig. 1a) and the Si_{Al} model (Fig. 1b) for α and β molecular orbital's are 3.93, 2.45 and 2.27, 4.22 eV. The total densities of states (TDOS) of these tubes show significant changes due to Si-doping in the gaps regions of the TDOS plots. Also, the band gaps showed differences between the two forms (Fig.1a and b). In comparison with the pristine model, the band gaps of the models shown in Fig.1a and b were reduced while their electrical conductance was increased, with the doping in the Si_N model having a stronger effect than the doping in the Si_{Al} model on the band gap of the AlNNT (Table 1).

To better understand the nature of the interaction in the Si-doped models, we studied the electronic energies of the models. The highest occupied molecular orbital (HOMO) and lowest unoccupied molecular orbital (LUMO) in the pristine, Si_N, and Si_{Al} models are plotted in Fig. 3. For the pristine model, the HOMO is distributed throughout the N atoms; whereas, the LUMO is localized at the center of the nanotube. For the Si_N and Si_{Al} models, the HOMO is highly localized in the Si-doped regions. The LUMO for the Si_N and Si_{Al} models is localized at the center of the nanotube except at the Si-doped regions which approve the significant changes of geometries are just for those atoms located in the nearest neighborhood of the Si-doped AlNNTs whereas those of other atoms remain almost unchanged.

The charge distribution can be explained by MEP calculations. We computed the MEP surfaces for pristine and in the Si-doped models. The MEP is the potential generated by the charge distribution of the molecule, which has been used to explore the chemical properties of several materials [18, 19]. The electrostatic potentials of boron nitride nanotubes (BNNTs) and carbon nanotubes (CNTs) have been theoretically studied by Politzer et al. [18]. They showed that the pristine of BNNTs have much stronger and more variable surface potentials than the CNTs and the B and N atoms are positively and negatively charged on outer surfaces of the BNNTs, whereas as shown by the MEP plots in Fig. 4, in the pristine (6,0) *zigzag* AlNNT, the aluminum atoms are positively charged (blue colors) and the N

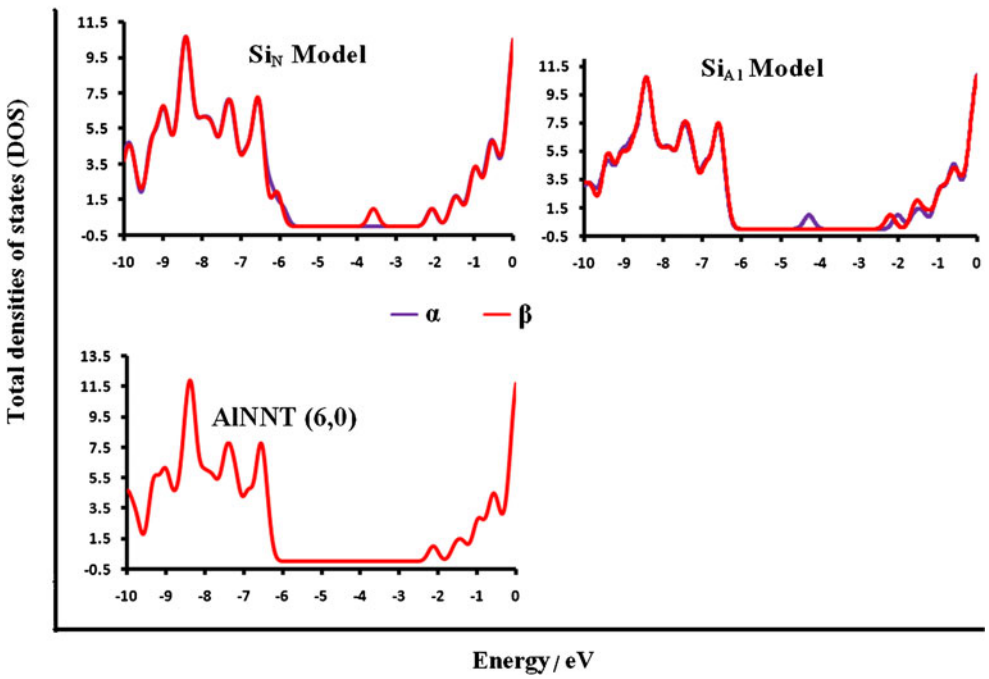

Fig. 2 Total densities of states (DOS) for different models of the AlNNTs

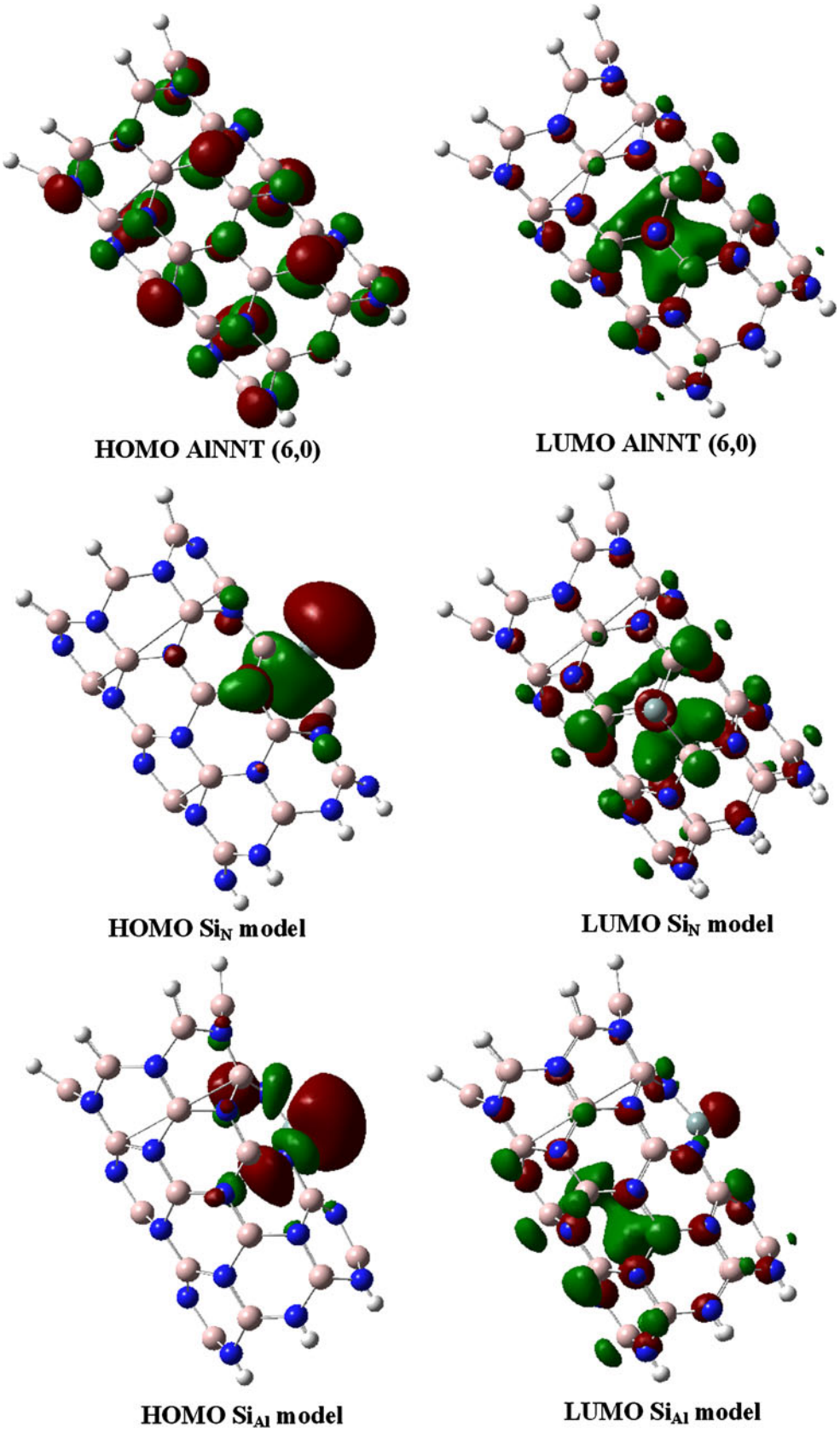

Fig. 3 HOMO and LUMO for different models of the AlNNTs

atoms are relatively negatively charged (yellow or red colors) in Al–N bonds of the pristine surface. It indicates that some charge is transferred from the Al atoms to the N ones resulting in an ionic bonding in AlNNT surface. On the other hand, in the Si_{Al}

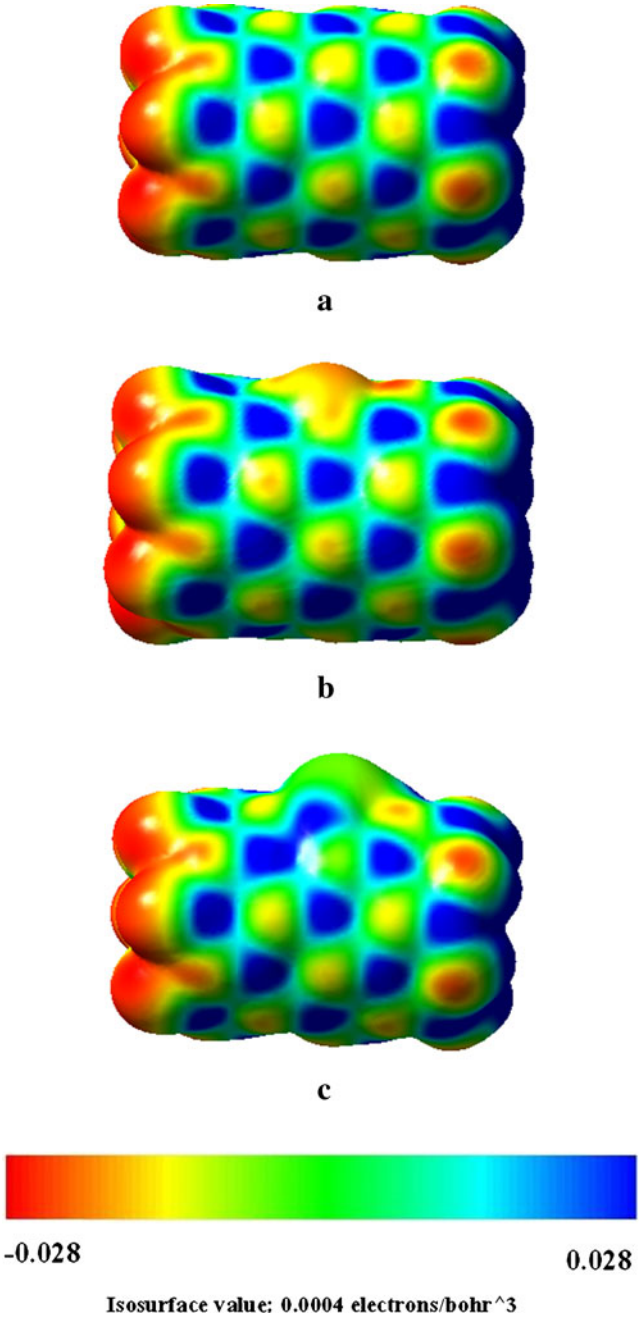

Fig. 4 Computed B3LYP/6-31G* electrostatic potentials on the molecular surfaces of (**a**) a pristine (6,0) AlNNT (**b**) a Si-doped (6,0) *zigzag* AlNNT in the Si_{Al} model (**c**) a Si-doped (6,0) *zigzag* AlNNT in the Si_N model. Color ranges are in a.u

model (Fig. 4b), the Si-doped regions negatively charged (red colors), whereas in the Si_N models (Fig. 4c), in the Si-doped regions, the electrostatic potential going from negative to neutral (green colors).

NMR parameters of the (6,0) zigzag AlNNT models

The NMR parameters including isotropic and anisotropic chemical shielding (CS^I and CS^A) parameters for the investigated (6,0) *zigzag* AlNNT models at the sites of various ^{27}Al and ^{15}N atoms are summarized in Table 2. In the pristine model of the (6,0) *zigzag* AlNNT, there are 30 Al and 30 N atoms in the considered model, and the NMR parameters are separated into five layers: 1–6, 7–12, 13–18, 19 – 24, and 25–30 (Table 2, Fig. 1c). In this model, the values of the NMR parameters in each group were the same; however, the results presented in Table 2 indicate that the calculated NMR parameters were not similar for the different groups, meaning that the CS parameters for the atoms of each layer have equivalent chemical environment and electrostatic properties. The CS^I parameters show the average value of the CS tensors, whereas the CS^A parameter indicates the orientations of the CS tensors at the atomic site [4]. Atoms Al1 to Al6, which are located at the edge of the (6,0) *zigzag* AlNNT (Al-terminated ends), have the smallest values of the CS^I and CS^A parameters among the Al atoms in the pristine model of the (6,0) *zigzag* AlNNT, whereas atoms N25 to N30, which are located at the edge of the (6,0) *zigzag* AlNNT (N-terminated ends), have the largest values of the CS^I parameters. The results show that the changes of values of CS^I parameters follow opposite directions for Al and N layers.

In Fig. 1a, i.e.; the Si_N model, atom N14 is doped by the Si atom. Thus, there are three Si–Al bonds instead of three Al-N bonds. Therefore, there are 30 Al and 29 N atoms in the considered model. The calculated results presented in Table 2 show that, the CS^I and CS^A values of atoms Al14, Al15, and Al20, which are directly bonded to the Si atom, show the most significant changes due to the Si-doping among the Al atoms of the Si_N model; the CS^I values of the atoms are decreased, whereas the CS^A values of the atoms are increased (see Table 2). Also, the changes in the values of the CS^I parameters for atoms Al19 and Al21, which are indirectly bonded to the Si atom, are notable. For other Al atoms of the model, changes of the CS^I and CS^A values of the Al atoms are almost negligible. Among the N atoms of Fig. 1a (Si_N model), the N7, N8, N9, N15, N20, and N21atoms, which are indirectly bonded to the Si atom, show the most significant changes due to the Si-doping among the N atoms of the Si_N model, the CS^I values of the atoms are decreased, whereas the CS^A values of the atoms are increased. For other N atoms of the model, the CS parameters of the atoms remain almost unchanged. In the original Al-N bonds, because of larger value of electronegativity of the N atom than the Al atom, the bonding electronic distribution is oriented to the N atom, whereas in the new Si-Al bonds, because of low electronegativity differences between the Al and Si atoms, the electronic distribution between two atoms is almost the same. This trend could well be proven by decrease of the values of the CS^I parameters and increase of the values of the CS^A parameters for the Al and N atoms of close to the Si-doped regions in the Si_N model.

In Fig. 1b, i.e.; the Si_{Al} model, atom Al15 is doped by the Si atom. Thus, there are three Si–N bonds instead of three Al-N bonds. Therefore, there are 29 Al and 30 N atoms in the considered model. The calculated results presented in Table 2 show that just, the CS^A values of atoms Al8, Al9, Al 14, and Al16, which are indirectly bonded to the Si atom, show the most significant changes due to the Si-doping among the Al atoms of the Si_{Al} model; the CS^A values of the atoms are increased, whereas the CS^I values of the atoms remain almost unchanged. For other Al atoms of the model, changes of the CS^I and CS^A values of the Al atoms are almost negligible. Among the N atoms of Fig. 1b (Si_{Al} model), the N9, N14, and N15 atoms, which are directly bonded to the Si atom, show the most significant changes due to the Si-doping among the N atoms of the Si_{Al} model, the CS^I values of the atoms are decreased, whereas the CS^A values of the atoms are increased. For other N atoms of the model, the CS parameters of the atoms remain almost unchanged. In the Si_{Al} model, because of almost same values of electronegativity of the Al and Si atoms, the bonding electronic distribution in Al-N and Si-N bonds are almost same. Therefore, this trend is agreement with the slight changes in CS^I and CS^A values of the Si_{Al} model with respect to the pristine (6,0) *zigzag* AlNNT. Comparison of the calculated NMR parameters in Fig. 1a, b shows that the electronic structure properties of Fig. 1a of the Si-doped (6,0) *zigzag* AlNNT where the N atom is doped by the Si atom (Si_N model) are more strongly influenced than those of Fig. 1b where the Al atom is doped by the Si atom (Si_{Al} model). According to these results, it could be suggested that the Si_N model is a more reactive material than the pristine or Si_{Al} model of the (6,0) *zigzag* AlNNT.

^{27}Al and ^{14}N electric field gradient tensors of the (6,0) zigzag AlNNT models

The NQR parameters at the sites of various ^{27}Al and ^{14}N nucleus for the optimized investigated (6,0) *zigzag* AlNNT models are summarized in Table 3. There are 30 Al and 30 N atoms in the considered models of *the* (6,0) zigzag AlNNT, and the NQR parameters are separated into five layers based on the similarity of the calculated electric field gradient (EFG) tensors in each layer. The results presented in Table 3 shows that the calculated NQR parameters are not similar for various nuclei; therefore, the electrostatic environment of the AlNNT is not equivalent along its lengths of the nanotube models. In Figs. 1, the Al1 (Al-terminated end) and N25 (N-terminated end) atoms indicates the position of the first layer, atoms Al7 and N19 shows the position of the second layer, atoms Al13 and N13 indicates the position of the third layer, atoms Al19 and N7 indicates the position of the fourth layer, atoms Al25 and N1 indicates the position of the fifth layer in the considered *zigzag* models. The Al1 (Al-tip) and N25 (N-tip) layers are placed at the end of the tubes and include Al and N atoms. In the (6,0) zigzag AlNNT models, the values of C_Q(^{27} Al1 and ^{14}N25) are the largest among the ^{27}Al and ^{14}N nucleus (Table 3), indicating greater orientation of the EFG tensor eigenvalues along the z-axis of electronic distribution at the sites of ^{27}Al and $^{14}N2$ nucleus. The electrostatic environment of atoms Al 1 and N25 are stronger than in the other layers along the length of the tube. Other research has shown that such nanotubes grow from their ends; hence, the properties of the end nuclei in nanotubes are important for their growth and synthesis [20, 21]. Therefore, in the AlNNTs the Al and N atoms located at the edge of the (6,0) zigzag nanotubes play important roles in determining the electronic behavior of the (6,0) zigzag AlNNTs, because the geometrical properties of this layer are different from those of the other layers. Comparison of the calculated C_Q (^{27}Al), C_Q (^{14}N), and η_Q parameters of the considered (6,0) zigzag AlNNT models shows that the electronic sites of the Al and N atoms of Fig. 1a, i.e., the Si_N model, exhibit greater changes than the Si_{Al} model in Fig. 1b with respect to the pristine model. Therefore, the NQR results presented in Table 3 shows that with the doping in the Si_N model having a stronger effect than the doping in the Si_{Al} model on the NQR of the AlNNT.This trend is in agreement with the changes in the NMR parameters and band gap of Fig. 1a (Si_N model), in comparison with the model of the pristine (6,0) zigzag AlNNT.

Quantum molecular descriptors of the (6,0) zigzag AlNNT models

The quantum molecular descriptors for the pristine (6,0) zigzag AlNNT, Si_N, and Si_{Al} models are summarized in Table 4. We observe that in the Si_N and Si_{Al} models, the energy gap (E_{LUMO} - E_{HOMO}) decreased. This lowering of energy gap in the Si doping process may be able to increase the reactivity of the models. The global hardness and ionization potential of the Si-doped AlNNT models decreases

Table 4 Quantum molecular descriptors in representative models of the (6,0) *zigzag* AlNNTs

Property	Si_N model		Si_{Al} model		Pristine
	α	β	α	β	
E_{HOMO}/eV	−5.92	−6.04	−4.28	−6.43	−6.42
E_{LUMO}/eV	−2.09	−3.59	−2.01	−2.21	−2.13
[E_{LUMO} -E_{HOMO}]/eV	3.93	2.45	2.27	4.22	4.29
[I=− E_{HOMO}]/eV	5.92	6.04	4.28	6.43	6.42
[A=− E_{LUMO}]/eV	2.09	3.59	2.01	2.21	2.13
[η=(I − A)/2]/eV	1.96	1.22	1.14	2.11	2.14
[μ=− (I+ A)/2]/eV	−4.00	−4.82	−3.14	−4.32	−4.28
[S=1/2η]/eV^{-1}	0.26	0.41	0.44	0.24	0.23
[ω=μ^2/2 η]/eV	4.08	9.52	4.32	4.42	4.28

I = ionization potential, A = electron affinity, η = Global hardness, μ = Chemical potential, and ω = electrophilicity

with a decrease in energy gaps of the models. Decrease in global hardness, energy gap, and ionization potential because of the Si doping process lowers the stability and increase the reactivity of the models. The electrophilicity index is a measure of electrophilic power of a molecule. The electrophilicity of the Si-doped AlNNT models are much further from the electrophilicity of the pristine model. Therefore, the Si doping process increases the electrophilicity of the models. The value of hardness, softness, electerophilicity, and chemical potential for the Si-doped AlNNT models differ from that of the individual tube. In the Si doping process, the capacity of the AlNNT models to attract electrons was diminished and the hardness of the Si-doped AlNNT models was decreased, which means decreased stability of the systems.

Conclusions

We studied the electronic structure properties including bond lengths, bond angles, tip diameters, dipole moments, band gaps, the quantum molecular descriptors, and NMR and NQR parameters of pristine and two Si-doped AlNNT models by means of DFT calculations. The calculated results showed that the effects of the Si dopant are important for the Al-N bond distances close to the Si-doped regions, whereas the values for other bonds do not show notable changes. Also, the average Al–N bond lengths are almost the same in the pristine (6,0) zigzag AlNNT and the Si_{Al} model, but different in the Si_N model due to the influence of the Si doping on the AlNNT. The binding energy (*BE*) for the Si_{Al} model is attractive, which is characteristic a chemisisorption process and denotes exothermic substitute, whereas for the Si_N model is not attractive and do not characterize a chemisisorption process and denotes endothermic substitute. The dipole moments of the Si-doped AlNNT structures showed slight changes due to the Si-doping with respect to the pristine model. In comparison with the pristine model, the band gaps of the Si_N and Si_{Al} models were reduced while their electrical conductance was increased, with the doping in the Si_N model having a stronger effect than the doping in the Si_{Al} model on the band gap of the AlNNT. The HOMO and LUMO of the models show that the significant changes of geometries are just for those atoms located in the nearest neighborhood of the Si-doped AlNNTs whereas those of other atoms remain almost unchanged. The NMR and NQR results show that, for the Si_N and Si_{Al} models, the electronic structure properties of the Si_N model are more strongly influenced than those of the Si_{Al} model, and the electronic sites of the Al and N atoms in the Si_N model show greater changes than in the Si_{Al} model due to the Si doping process, which shows the Si_N model is a more reactive material than the pristine or Si_{Al} model of the (6,0) zigzag AlNNTs. Also, decrease in global hardness, energy gap, and ionization potential because of the Si doping process lowers the stability and increase the reactivity of the models. The important results can help in production of solid-state devices and to better understand the mechanism of action of doping in nanotubes and also design further molecules with better reactivity.

Acknowledgments This work was financially supported by Islamic Azad University, Azadshahr Branch.

References

1. Strite S, Morkoc H (1992) J Vac Sci Technol B 10:1237
2. Jain C, Willander M, Narayan J, van Overstraeten R (2000) J Appl Phys 87:965
3. Ruterana P, Albrecht M, Neugebauer J (2003) Nitride Semiconductors: Handbook on Materials and Devices. Wiley, New York
4. Bovey FA (1988) Nuclear Magnetic Resonance Spectroscopy. Academic Press, San Diego
5. Das TP, Han EL (1958) Nuclear Quadrupole Resonance Spectroscopy. Academic Press, New York
6. Baei MT, Sayyed Alang SZ, Moradi AV, Torabi P (2012) J Mol Model 18:881–889
7. Baei MT, Moradi AV, Torabi P, Moghimi M (2011) Monatsh Chem 142:783–788
8. Baei MT, Moradi AV, Moghimi M, Torabi P (2011) Comput Theor Chem 967:179–184
9. Baei MT, Moradi AV, Torabi P, Moghimi M (2011) Monatsh Chem 142:1097–1104
10. Mirzaei M, Seif A, Hadipour NL (2008) Chem Phys Lett 461:246–248
11. Chattaraj PK, Sarkar U, Roy DR (2006) Chem Rev 106:2065–2091
12. Hazarika KK, Baruah NC, Deka RC (2009) Struct Chem 20:1079
13. Parr RG, Szentpaly L, Liu S (1999) J Am Chem Soc 121:1922–1924
14. Baei MT, Moghimi M, Torabi P, Moradi AV (2011) Comput Theor Chem 972:14–19
15. Baei MT (2011) Monatsh Chem. doi:10.1007/s00706-011-0673-5
16. Pyykkö P (2001) Mol Phys 99:1617–1629
17. Schmidt M et al (1993) J Comput Chem 14:1347–1363
18. Peralta-Inga Z, Lane P, Murray JS, Boyd S, Grice ME, O'Connor CJ, Politzer P (2003) Nano Letters 3(1):21–28
19. Politzer P, Lane P, Murray JS, Concha MC (2005) J Mol Model 11 (1):1
20. Hou S, Shen Z, Zhang J, Zhao X, Xue Z (2004) Chem Phys Lett 393:179
21. Bengu E, Marks LD (2001) Phys Rev Lett 86:2385–2387